

Stability of the synchronization manifold in nearest neighbors non identical van der Pol-like oscillators

R. Yamapi

*Fundamental Physics Laboratory, Group of Nonlinear Physics and Complex System,
Department of Physics, Faculty of Science, University of Douala,
Box 24 157 Douala, Cameroon, Email address: ryamapi@yahoo.fr*

H. G. Enjieu Kadji

*Institute for Development, Aging and Cancer, Tohoku University 4-1 Seiryochō,
Aobaku, Sendai 980-8575, Japan, Email address: henjieu@yahoo.com*

G. Filatrella

*Laboratorio Regionale SuperMat, CNR/INFM Salerno and Dipartimento di Scienze Biologiche ed Ambientali,
Università del Sannio, via Port'Arsa 11, I-82100 Benevento, Italy, Email address: giofil@sa.infn.it*

(Dated: January 19, 2010)

We investigate the stability of the synchronization manifold in a ring and an open-ended chain of nearest neighbors coupled self-sustained systems, each self-sustained system consisting of multi-limit cycles van der Pol oscillators. Such model represents, for instance, coherent oscillations in biological systems through the case of an enzymatic-substrate reaction with ferroelectric behavior in brain waves model. The ring and open-ended chain of identical and non-identical oscillators are considered separately. By using the Master Stability Function approach (for the identical case) and the complex Kuramoto order parameter (for the non-identical case), we derive the stability boundaries of the synchronized manifold. We have found that synchronization occurs in a system of many coupled modified van der Pol oscillators and it is stable even in presence of a spread of parameters.

I. INTRODUCTION

During the last decades, the emergence of collective dynamics in large networks of coupled units has been investigated in disciplines such as physics, chemistry, biology and ecology. In particular, the effect of synchronization in systems of coupled oscillators nowadays provides a unifying framework for different phenomena observed in nature (for some reviews see [1–3]). Recently, complex networks have provided a challenging framework for the study of synchronization of dynamical units, based on the interplay between complexity in the overall topology and local dynamical properties of the coupled units. A key problem is to assess conditions that guarantee the stability of the synchronous behavior for a network topology with some class of coupling configuration. To determine such conditions, many methods have been developed and among these, the so-called Master Stability Function (MSF) [4]. Indeed, the MSF approach was originally introduced for arrays of coupled oscillators [4], and it has been later extended to the case of a complex networks of dynamical systems coupled with arbitrary topologies [5–8]. We will use the MSF to investigate the stability boundaries of the synchronization manifold in a ring and an open-ended chain of self-sustained oscillators described by coupled multi-limit cycles van der Pol oscillators (MLC-vdPo) that might display birhythmicity, a mathematical model for instance suitable for some enzymatic substrate reaction with ferroelectric behavior in a brain waves model [9], as well as in other biochemical models [10].

Limit cycles are the fascinating objects in natural sciences where nonlinear kinetics due to feedback and cooperativity leads to instability of the fix point and evolves towards periodic sustained oscillations. Examples are abundant, with periods ranging from cardiac rhythms of seconds, glycolysis over minutes, circadian oscillations over the 24 hours, while epidemiological oscillations extend over the years [11–13]. Compared to the classical van der Pol system that possesses only one stable limit cycle, the MLC-vdPos has the advantage to better explain some biological processes, through its possibility of showing up multi limit cycles oscillatory states [14]. Thereby, we aim to understand how a large (but finite) number of interacting MLC-vdPos will behave collectively, given their individual dynamics and a corresponding coupling topology. We will investigate two oscillators coupling topology, a ring and an open-ended chain, both with nearest neighbors coupling. Indeed, such couplings are of paramount importance since they occur in many applications, both in natural and artificial systems, that involve the problem of coordination of multiple agents (circadian rhythm, contraction of coronary pacemaker cells, firing of memory neurons in the brain, superconducting Josephson junction arrays, design of oscillator circuits, sensor networks)[15–20]. We will show that synchronization also occurs in the system of many coupled modified van der Pol oscillators and it is stable even in presence of a spread of parameters.

The organization of the paper is the following: Section II deals with the description of the model under consideration. In Section III, the stability boundaries of the synchronized states in a ring of identical MLC-vdPos are retrieved through

the MSF approach, and numerical simulations are used to validate and complement the results. Section IV addresses the ring of non-identical MLC-vdPos, while Section V considers the stability of synchronization manifold in a chain of open-ended nearest neighbors coupled identical and non-identical self-sustained oscillators. Finally, Section VI is devoted to the conclusions.

II. THE SELF-SUSTAINED MODIFIED VAN DER POL OSCILLATOR

The modified van der Pol oscillator is described by the following nonlinear differential equation (in non-dimensional form)

$$\ddot{x}_c - \mu(1 - x_c^2 + \alpha x_c^4 - \beta x_c^6)\dot{x}_c + x_c = 0. \quad (1)$$

(Overdots stand for the derivative with respect to time). Such model, that exhibits an extremely rich bifurcation behavior, was proposed by Kaiser [14], and describes many dynamical systems, ranging from physics, biochemistry to engineering. When employed to model biochemical systems, namely the enzymatic-substrate reaction, \dot{x}_c represents the rate of change of the number of excited enzyme molecules and x_c in Eq. (1) is proportional to the population of enzyme molecules in the excited polar state. The quantities α and β are positive parameters which measure the degree of tendency of the system to a ferroelectric instability compared to its electric resistance, while μ is the parameter that tunes nonlinearity [21]. The nonlinear dynamics and the synchronization process of two such systems have been investigated recently [21, 22], while Ref. [23] considers its dynamics and active control to find that chaos can be tamed for an appropriate choice of the coupling parameters. Coupled van der Pol oscillators have been considered in [24–26]. Depending to the values of the parameters β and α , Eq. (1) can lead to one or three limit cycles. When three limit cycles are obtained, two of them are stable and one is unstable, a condition for birhythmicity [10]: The unstable limit cycle represents the separatrix between the basins of attraction of the two stable limit cycles (see [21]). We will avoid such region for simplicity, so the uncoupled elements are monorhythmic. We show in Fig.1 the region of existence of birhythmicity in the two parameter phase space (β - α) [21, 22].

III. THE RING OF IDENTICAL SELF-SUSTAINED OSCILLATORS

A. The model

When the coupling is realized through a ring topology, *i.e.* with periodic boundary conditions, the model is described by the following set of dimensionless nonlinear differential equations:

$$\begin{aligned} \ddot{x}_1 - \mu(1 - x_1^2 + \alpha x_1^4 - \beta x_1^6)\dot{x}_1 + x_1 &= K(x_2 - 2x_1 + x_N), \\ \ddot{x}_\nu - \mu(1 - x_\nu^2 + \alpha x_\nu^4 - \beta x_\nu^6)\dot{x}_\nu + x_\nu &= K(x_{\nu+1} - 2x_\nu + x_{\nu-1}), \quad \nu = 2, 3, \dots, N-1, \\ \ddot{x}_N - \mu(1 - x_N^2 + \alpha x_N^4 - \beta x_N^6)\dot{x}_N + x_N &= K(x_1 - 2x_N + x_{N-1}). \end{aligned} \quad (2)$$

Here, K stands for the diffusive (nearest-neighbor) coupling strength. The physical meaning of the variables depends on the nature of the system described by such a ring. For instance, let us consider the case of a ring of immobilized self-sustained enzymes that minimize the cost of production by permitting repeated use of the enzymes and substantially increases the stability of the enzyme reactions themselves [27]. We propose to describe the coupling between cells by means of the diffusion of the solute concentration, so K is proportional to the difference in the concentration. Since within each self-sustained system there are promoters (positive direction of solute flow) and inhibitors (negative direction of solute flow) that determine the direction of the solute flow, it follows that the coupling coefficient K can be either negative or positive.

The system of diffusive coupling occurs in many complex systems. For instance, the ring of multi-limit cycles oscillators is of interest to construct hypotheses on the *in vivo* enzymes behavior when they possess more than one stable limit cycle. A ring of the MLC-vdPos can therefore serve as a simple model of a biological oscillator. The set of equations (2) can also be exploited in electronics engineering as a network of parallel microwaves oscillators [28, 29]: Multiple limit cycles can be obtained from a classical van der Pol oscillator with hysteresis in the inductance [30]. Since we are interested in the synchronization manifold, the following subsection deals with the stability of the synchronous states in the ring of mutually coupled identical self-sustained oscillators.

B. Stability of the synchronization manifold

We aim now to determine the stability of the synchronous state in the system (2) of self-sustained oscillator requiring that each of the perturbed trajectories returns to its original limit cycle. We are therefore interested in the bifurcations from the state that resides on a synchronization manifold denoted by $\mathcal{M} = \{(x_1, y_1) = (x_2, y_2) = \dots = (x_N, y_N)\}$. In order to rewrite Eqs. (2) as set of flows, we have introduced a new variable $y_\nu = \dot{x}_\nu$; with such new variables the corresponding dynamic equations read:

$$\begin{aligned} \dot{x}_\nu &= y_\nu, \\ \dot{y}_\nu &= \mu(1 - x_\nu^2 + \alpha x_\nu^4 - \beta x_\nu^6)y_\nu - x_\nu + K(x_{\nu+1} - 2x_\nu + x_{\nu-1}), \quad \nu = 1, 2, \dots, N. \end{aligned} \quad (3)$$

To verify the stability of the synchronization manifold \mathcal{M} we make use of the MSF approach [4, 31]. Thereby, let \mathbf{X}^i be the two-dimensional vector of the dynamical variables of the i^{th} unit, $\mathbf{H} : R^2 \rightarrow R^2$ an arbitrary function describing the coupling between each unit variables. Thus, the dynamics of the i^{th} unit is rewritten as a function of the $2 \times N$ column vector state \mathbf{X}^i as

$$\dot{\mathbf{X}}^i = \mathbf{F}(\mathbf{X}^i) + K \sum_j^N G_{ij} \mathbf{H}(\mathbf{X}^j), \quad i = 1, 2, \dots, N, \quad (4)$$

where $\mathbf{X}^i = [x_i, y_i]^T$, $\mathbf{F}(\mathbf{X}^i) = [y_i, \mu(1 - x_i^2 + \alpha x_i^4 - \beta x_i^6)y_i - x_i]^T$, and the function \mathbf{H} is defined through the matrix

$$\mathbf{E} = \begin{pmatrix} 0 & 0 \\ 1 & 0 \end{pmatrix},$$

by $\mathbf{H}(\mathbf{X}^i) = \mathbf{E}\mathbf{X}^i$. $G_{ij} \in R$ are the elements of the $N \times N$ symmetry connectivity matrix \mathbf{G} defined as

$$\mathbf{G} = \begin{pmatrix} -2 & 1 & 0 & \dots & 1 \\ 1 & -2 & 1 & \dots & 0 \\ 0 & 1 & -2 & \dots & 0 \\ \vdots & \vdots & \vdots & \ddots & \vdots \\ 1 & 0 & \dots & 1 & -2 \end{pmatrix}.$$

Since the ring is made of identical self-sustained oscillators, the evolution function $F(\mathbf{X}_i)$ in Eq. (4) is the same for all ring node. This ensures the existence of an invariant set $(x_i(t), y_i(t)) = (x_s(t), y_s(t))$, $\forall i$, representing the complete synchronization manifold \mathcal{M} . Following the MSF scheme [1, 2, 4], the stability of the resulting dynamical states can be determined by letting

$$\begin{aligned} x_\nu(t) &= \delta x_\nu(t) + x_s(t), \\ y_\nu(t) &= \delta y_\nu(t) + y_s(t), \end{aligned}$$

and linearizing equations (4) around the periodic limit-cycle state (x_s, y_s) . This approach leads to the following equation:

$$\delta \dot{\mathbf{X}}(t) = [1_N \otimes \mathbf{JF}(\mathbf{X}_s) + K\mathbf{G} \otimes \mathbf{JH}(\mathbf{X}_s)]\delta \mathbf{X}(t), \quad (5)$$

where \otimes stands for the direct product between matrices. J denotes the Jacobian operator and the $2 \times N$ column vector $\delta \mathbf{X}^i(t) = (\delta x_i(t), \delta y_i(t))$ is the deviation of the i^{th} vector state from the synchronization manifold. We have used the definitions $\mathbf{H}(\mathbf{X}^i) = \mathbf{E}\mathbf{X}^i$, and $\mathbf{JH} = \mathbf{E}$.

A necessary condition for stability of the synchronization manifold is that the set of $(N-1) \times 2$ Lyapunov exponents that corresponds to phase space directions transverse to the 2-dimensional hyperplane $\mathbf{X}^i(t) = \mathbf{X}_s(t)$ should be entirely made of negative values [4, 31]. The arbitrary state $\delta \mathbf{X}(t)$ can be written as $\delta \mathbf{X}(t) = \sum_{i=1}^N v_i \otimes \xi_i(t)$ with $\xi_i(t) = (\xi_{i,1}(t), \xi_{i,2}(t))$. If one applies $[v_j]^T$ (γ_i and $[v_i]$ are the set of real eigenvalues and the associated orthonormal eigenvectors of the matrix \mathbf{G}) to the left side of each equation in (5), one finally obtains the following set of N variational equations

$$\dot{\xi}_k(t) = [\mathbf{JF}(\mathbf{X}_s) + K\gamma_k \mathbf{JH}(\mathbf{X}_s)]\xi_k(t), \quad k = 0, 1, 2, \dots, N-1. \quad (6)$$

The eigenvalues γ_k of \mathbf{G} are given by $\gamma_k = -4\sin^2(\pi k/N)$ [4, 32]. Let us remark that the mode $k = 0$ is the "slower" or uniform mode, while $k = N - 1$ is the "faster" or more rapidly oscillating (in the momentum space) mode. Each mode k in Eq. (6) corresponds to a set of 2 conditional Lyapunov exponent λ_k^j ($j = 1, 2$) along the eigenmode related to a specific eigenvalue γ_k . Eqs. (6) enable to compute the maximum Lyapunov exponent λ_k^{max} of each mode k as a function of the coupling parameter K . In the following, we will use the parametrical behavior of the largest of such exponents $\Lambda(K)$, called MSF, to determine the stability boundaries of the synchronization states in the ring of coupled self-sustained systems.

C. Numerical simulations

We now address the numerical computation of the Lyapunov exponents and then the MSF Λ , by solving the equations of motion (1) and the variational equations (6), with a fourth-order *Runge-Kutta* algorithm. The parameters used are representative of the monorhythmic solutions: $\mu = 0.1$, and in (i): $\alpha = \beta = 0.1$, while in case (ii) we set $\alpha = 0.114$, $\beta = 0.005$.

When the coupling coefficient is turned off (*i.e.* $K = 0$), the self-sustained systems are uncoupled and the corresponding MSF is $\Lambda(K = 0) = 0$. For $K \neq 0$, and for a given ring size N , the MSF $\Lambda(K)$ will enable us to derive the range of the coupling parameter K in which the transverse *Fourier* modes are stable, and therefore each oscillator of the ring exhibits the same dynamical states. The behavior of the MSF as a function of the coupling K and the number of oscillators N is plotted in Fig. 2. Starting from large negative K values, the first domain is the unstable synchronization domain (D_{US}) in which there is some positive transverse Lyapunov exponent. The boundaries slowly change with the number N of oscillators (see Table 1); when synchronization is not observed, all the modes are on the transverse manifold where variations transverse to the synchronization manifold do not decay; all or some of the transverse *Lyapunov* exponents are positive, *i.e.* $\lambda_k^{max} > 0$.

N	Domains of coefficient K for unstable synchronization (D_{US})	N	Domains of coefficient K for unstable synchronization (D_{US})
4	$]-\infty; -0.25[\cup]-0.02; 0[\cup]0; +0.005[$	60	$]-\infty; 1.93[$
10	$]-\infty; -0.25[\cup]-0.028; 0[\cup]0; 0.055[$	70	$]-\infty; 2.63[$
20	$]-\infty; -0.25[\cup]-0.11; 0[\cup]0.0; 0.21[$	80	$]-\infty; 3.0[$
30	$]-\infty; 0.48[$	90	$]-\infty; 4.36[$
40	$]-\infty; 0.86[$	100	$]-\infty; 5.38[$
50	$]-\infty; 1.34[$		

Table 1: Range of coupling values for unstable synchronous state in the ring of oscillators with one limit-cycle. Parameters of the system are $\mu = 0.1$, $\alpha = 0.1$, $\beta = 0.1$.

In other words, the *Fourier* modes increase continuously or possess a bounded oscillatory behavior and one never observes stable synchronization in the ring for such a choice of the coupling strength. It should be underlined that the region D_{US} where unstable synchronization is found, can be divided in two sub-domains: the first sub-domain corresponds to the non-synchronization phenomena, while the second sub-domain corresponds to partial synchronization. For example for $N = 4$, in the first sub-domain ($K \in]-\infty; -0.25[$), any perturbed trajectory leads the oscillators to continuously drift away from their original limit cycles. In the second sub-domain, ($K \in]-0.02; 0[$) although perfect synchronization is not observed, there is some tendency towards co-operative behavior, as will be shown in Sect. IV by means of the Kuramoto order parameter.

It appears that as the coupling coefficient K increases from $-\infty$, where the ring of coupled self-sustained systems is on the unstable synchronized states (and therefore all Lyapunov exponents are positive), the mode $k = 1$ is the first one to move from the unstable to the stable domain. On the other hand, $k = N/2$ is the last mode that leaves from the unstable domain to enter the stable state. At this point, the ring is on the stable synchronized state; when the coupling coefficient K is further increased, the mode $k = 1$ is the first mode to move from the stable domain to the unstable one, and the mode $k = N/2$ is the last one. For the case of the positive coupling coefficient K , the reverse situation is observed: the $k = N/2$ mode is the first to become stable. Also in the case (ii) with $\alpha = 0.114$ and $\beta = 0.005$, is found a similar behavior.

Since from a biological point of view, negative and positive values of the coupling strength refer to inhibitory and excitatory process, respectively, one can conclude the following: The instability of a synchronization process within a system of inhibitory ($K < 0$) cells is driven by the slowest, or lower k , mode. On the other hand, when a system is made of excitatory ($K > 0$) cells, the instability of the process is initiated through the fastest, or higher k , mode.

Fig. 3 shows the stability diagram in the (N, K) plane, *i.e.* it displays the border between the two main dynamical states. We have found with the MSF method that the number of units strongly affects the stability boundaries of the synchronization process in the ring. In particular, when $N > 30$, there is no domain of stable synchronization for

negative values of the coupling coefficient K . It is important to notice that Eqs. (6) have been linearized around the stable orbit. In order to check the validity of the above semi-analytical results, we have numerically solved Eqs. (2). Numerically, the stable synchronization state is achieved if all the oscillators of the system are in synchrony. This means that the synchronized state defined by the N constraints $(x_1, y_1) = (x_2, y_2) = (x_3, y_3) = \dots = (x_N, y_N)$ (within some precision or tolerance h) is in the synchronization manifold and therefore the stability of the synchronization process is ensured. The numerical synchronization criterion is defined as the sum of the absolute deviations from each oscillator respect to all other, and dividing such sum for the number of terms:

$$\frac{1}{N(N-1)} \sum_{i \neq j} |x_i - x_j| < h, \quad \forall(i, j). \quad (7)$$

It should be underlined that this numerical synchronization criterion gives an insight about perfect synchronization in the ring but does not tell anything about other types of dynamical behavior related to stable synchronization. In some regions where stable synchronization is expected from MSF analysis, one can instead observe unstable synchronization in the full model (2). The discrepancy depends upon the choice of initial conditions and the number of the self-sustained oscillators which are taken into account during the process. The neglected nonlinear terms give rise to nonlinear contributions that apparently increase with increasing the coupling K , thus explaining the discrepancy between the MSF method and the numerical simulations. From the criterion (7), we have obtained some results that depend on the number N . In particular we have noticed that increasing the number of oscillators the domain of stability of all modes shrinks. For instance, increasing the number of oscillators from $N = 6$ to $N = 8$ in Fig. 3(ii) the Lyapunov exponents associated to each mode become positive for a lower value of the coupling constant K : the first mode becomes unstable for $K > -0.014$ when $N = 6$, for $K > -0.019$ for $N = 7$, and for $K > -0.024$ for $N = 8$. An analogous behavior is observed for the other modes.

Both full synchronized states and no synchronization can be found in Fig. 3, where we also display the comparison between analytical and numerical results. One also finds some domains obtained only from numerical simulation that do not match with the MSF stability condition. It is important to notice that this gap depends upon the choice of the precision or tolerance h . In fact, given the accuracy of the numerical integration, if h is too small ($h \ll 10^{-6}$) one would never observe synchronization, while for too a large h ($h \gg 10^{-6}$) synchronization would appear as a spurious effect, so it is necessary to determine an appropriate value of the parameter h as a function of the accuracy of the numerical scheme, a value that we have estimated for our scheme to be $h \simeq 10^{-6}$. To circumvent such difficulty (and arbitrariness) we will suggest in Sect. IV another tool to detect synchronization, the Kuramoto order parameter.

Figs. 4 and 5 show space-time-amplitude diagrams that display the behavior for two values of the coupling parameter K in the unstable or no-synchronization (US) and stable synchronization (SS) domains. For the unstable domain, Fig. 4 shows the time evolution for $(N, K) = (30, -0.2)$ and $(N, K) = (50, -0.05)$, where no synchronization is found in the ring. Considering the domain of stable synchronization, we display in Fig. 5 for $(N, K) = (20, 0.6)$ and $(N, K) = (50, 1)$ the process of entrainment of the oscillators in the ring.

IV. THE RING OF NONIDENTICAL COUPLED OSCILLATORS

The understanding of the collective dynamics of synchronization processes occurring in living organisms is a paramount task of formidable difficulty. One reason is that in a realistic description of such systems, even within the same species, oscillators are made of non identical elements. Although not explicitly considered in this work, real systems are also always subject to noise in the form of fluctuations associated with dissipation, as well as in the form of random force due to the external environment. We will, however, focus our attention on quenched disorder, or non identical oscillators that can be modelled with a spread of the characteristic parameters. For example, a ring of nonidentical oscillators is useful to investigate calcium dynamics in pancreatic acinar cells [33] as well as other complex networks [34]. In the case where Eq.(2) is used to model biological systems of immobilized enzymes, the interpretation of the parameters μ , α and β requires that they can vary from site to site, according to the tendency degree of the oscillator to possess a ferroelectric behavior and also to the conductivity of the medium [21]. This leads to the possibility to have nonidentical biological oscillators, or to a ring of nonidentical coupled systems described by the following equations, where α and β are constant, while μ is not:

$$\begin{aligned} \ddot{x}_1 - \mu_1(1 - x_1^2 + \alpha x_1^4 - \beta x_1^6)\dot{x}_1 + w_1^2 x_1 &= K(x_2 - 2x_1 + x_N), \\ \ddot{x}_\nu - \mu_\nu(1 - x_\nu^2 + \alpha x_\nu^4 - \beta x_\nu^6)\dot{x}_\nu + w_\nu^2 x_\nu &= K(x_{\nu+1} - 2x_\nu + x_{\nu-1}), \quad \nu = 2, \dots, N-1, \\ \ddot{x}_N - \mu_N(1 - x_N^2 + \alpha x_N^4 - \beta x_N^6)\dot{x}_N + w_N^2 x_N &= K(x_1 - 2x_N + x_{N-1}). \end{aligned} \quad (8)$$

We recall that μ_ν are positive coefficients; they measure the dissipative strength and are smaller than unity. w_ν is the frequency of the associate linear oscillator ($\mu_\nu = 0$) and depends upon the site. The nonlinear terms play the role of amplitude-dependent dissipation and provide a self-sustaining mechanism for the perpetual oscillation. For the original biological system [21, 35], μ_ν can be expressed as function of the parameters of the systems as follows

$$\mu_\nu = \frac{\kappa^2 - \sigma^2}{w_{o\nu}} = \frac{18}{5} \alpha w_{o\nu} \kappa^2, \quad (9)$$

where $w_{o\nu}$ are the frequencies of the periodic enzyme-substrate reaction and can be determined by the recombination and attraction coefficients γ_ν, ξ_ν as $w_{o\nu} = \sqrt{\gamma_\nu \xi_\nu}$ [21]. ξ_ν is the decay rate of each excited enzymes to the ground (or weakly polar) state and γ_ν the range attraction of the substrate particles due to the autocatalytic reactions. From Frölich ideas, we may suppose that in large regions of the system of proteins, substrates, ions and structured water are activated by the chemical energy available from substrate enzyme reactions [36]. Thus, chemical oscillations in the number of substrate and activated enzyme molecules with a very low frequency $w_{o\nu}$ might be carried out around the equilibrium state [35]. κ (obtained through a nonlinear dielectric contribution) is the coefficient proportional to the macroscopic polarization and the time dependent number of the excited enzyme molecules [35]. It can be chosen in the interval $1 < \kappa < 5$. σ is viewed as a coefficient of relaxation term of electric resistances against the systems tendency to become ferroelectric. We assume that the frequency $w_{o\nu}$ is chosen as: $w_{o\nu} = 1 + \Delta w_o (\zeta_\nu - \frac{1}{2})$ (ζ_ν is a uniform random variable less than the unity and Δw_o a disorder parameter). We also assume that the natural frequencies w_ν are uniformly distributed around 1: $w_\nu = 1 + \Delta w (\zeta_\nu - \frac{1}{2})$. For simplicity, to avoid a new parameter, we take the spread of the recombination frequencies Δw_o and of the natural frequencies Δw to be the same: $\Delta w_o = \Delta w$. According to the analytical expression the amplitudes A and frequencies Ω_ν of the limit-cycles established in Ref.[21], the periodic solution for each oscillator is approximately described by

$$x_\nu(t) = A \cos \Omega_\nu t \quad (10)$$

where the amplitude A and the frequencies Ω_ν for the MLC-vdPo (1) are derived through the following equations:

$$\frac{5\beta}{64} A^6 - \frac{\alpha}{8} A^4 + \frac{1}{4} A^2 - 1 = 0, \quad (11(a))$$

$$\Omega_\nu = w_\nu + \frac{\mu^2}{w_\nu} \left\{ \frac{1580\beta}{393216} A^{12} - \frac{738\alpha\beta}{99024} A^{10} + \left(\frac{72\alpha^2 + 309\beta}{768} \right) A^8 - \left(\frac{64\alpha - 219\beta}{6144} \right) A^6 + \left(\frac{16\alpha + 3}{384} \right) A^4 - \frac{3}{64} A^2 \right\} + O(\mu^3). \quad (11(b))$$

We note that only the frequencies Ω_ν are modified by the disorder parameter Δw_o , while the amplitude A of the orbit does not change. Thus, each self-sustained system in the ring exhibits a different frequency, the amplitude, see Eq. (11(a)), only depends upon the α and β parameters, which are fixed here. The self-sustained oscillators with nonidentical μ_ν consist therefore of oscillators with nonidentical natural frequencies Ω_ν , that are a function of the physical parameters μ_ν , α , β , while the amplitude A of the limit-cycles is unchanged [21]. Therefore in the uncoupled limit approximated by the harmonic oscillations, see Eq.(10), each oscillator is completely described by a phase $\delta_\nu = \cos^{-1}(x_\nu(t)/A)$ and amounts to a rotator. It is therefore tempting to monitor the rotators through the phases δ_ν analogously to the Kuramoto model [37–39], a paradigm for coupled rotators and already employed to investigate globally coupled van der Pol oscillators [40]. Synchronization of the nonidentical oscillators (8) can be revealed by means of the Kuramoto order parameter R defined as [37–39]:

$$R = \frac{1}{N} \sum_{j=1}^N e^{i\delta_j}. \quad (12)$$

For a completely disordered steady-state one gets (for very large N) $R \simeq 0$, while $R \simeq 1$ corresponds to phase synchronization. The advantage to employ such parameter R is that it is possible to measure the degree of synchronization, or, roughly speaking, the fraction of synchronized oscillators in the intermediate cases of partial synchronization, for which the parameter R will reach a value $0 < R < 1$. So the Kuramoto order parameter R is capable to describe also states where condition (7) is not satisfied, but nevertheless the oscillators exhibit some tendency to behave coherently. The interest to determine the tendency of nonidentical systems to behave synchronously is almost ubiquitous, from laser arrays [41] to people walking on a bridge [42], or Josephson arrays [43]. For instance in the case of Josephson oscillators it has been speculated that the analysis of the Kuramoto order parameter (12) is useful to predict the

fraction of coherently working electronic elements, and therefore the efficiency of the devices [16, 44, 45]. Here we will use the Kuramoto order parameter in the same spirit: as a diagnostic tool to measure the capability of the oscillators to synchronize in spite of the differences in the single oscillators frequencies. In order to look at the qualitative picture of the dynamical states of oscillators under the influence of diffusive coupling, we have plotted in Fig. 6 the Kuramoto order parameter as a function of the coupling parameter K for several different finite number N of oscillators, as analyzed for instance in Ref. [46]. From Fig. 6, it can be noticed that full synchronization occurs mainly for $K > 0$, as expected from MSF analysis, although the Kuramoto order parameter allows an analysis of the partial synchronization (corresponding to a state - analogous to clustering - where the maximum Lyapunov exponent is positive, but not all modes are unstable [47]) that occurs in the region where full synchronization is unstable, see Sect. III. Therefore, this finding suggests that in the case of non-identical oscillators, excitatory coupling is more suitable to achieve coherent oscillations when compared to the inhibitory coupling ($K < 0$). It can be noticed that synchronization in presence of disorder is not achieved for negative K values as we show on Fig. 7 for an enlargement around low K values. From the Kuramoto order parameter (12), the following results have been obtained for $N = 6$, $N = 10$, $N = 20$ and $N = 30$. When the ring is composed of $N = 6$ nonidentical coupled oscillators, the phase synchronization state is achieved for $K \geq 1.6$. As the number of nonidentical oscillators in the ring increases, one still observes two main dynamical states but for different ranges of K , and in general the degree of synchronization decreases when the number of oscillators is increased. In the case of a ring composed of $N = 10$ and 20 nonidentical oscillators, full synchronization is obtained approximately in the range $K > 3.6$ and $K > 10.5$, respectively. For $N = 30$ oscillators in the ring, the oscillators are fully synchronized only for $K > 26.0$.

It is also interesting to compare the result of the Kuramoto order parameter analysis in Fig. 7 with the MSF analysis of Fig. 3. In this enlargement it is clear that disorder ($\Delta\omega_o = 0.05$) induces an enlargement of the desynchronization region around $K = 0$. For instance for $N = 10$ while the uniform oscillators are not synchronized only in the narrow region $-0.028 < K < 0.005$, after which there is a range of perfect synchronization (see also Table 1), from the simulation of disordered oscillators in Fig. 7 it is evident that there is a much more extended region of partial synchronization. Nevertheless it is clear that the qualitative behavior is the same in Fig. 3 and Fig. 6: the region unfavorable to synchronization around low K values clearly increases increasing the number N of oscillators in both the ordered and disordered cases.

The behaviors of the space-time-amplitude in the partially synchronized state and in the fully synchronous motion are similar to the patterns shown in Figs. 4 and 5. The ring of nonidentical oscillators capability to give rise to synchronization is represented in Table 2.

N	Domains of K for synchronization (i)	Domains of K for synchronization (ii)
2	$[0.4; +\infty [$	$[0.2; +\infty [$
3	$[0.6; +\infty [$	$[0.3; +\infty [$
4	$[0.7; +\infty [$	$[0.6; +\infty [$
5	$[1.0; +\infty [$	$[0.7; +\infty [$
6	$[1.3; +\infty [$	$[0.8; +\infty [$
8	$[2.4; +\infty [$	$[1.3; +\infty [$
10	$[3.6; +\infty [$	$[1.6; +\infty [$
15	$[7.2; +\infty [$	$[4.1; +\infty [$
20	$[12.8; +\infty [$	$[7.6; +\infty [$
25	$[19.4; +\infty [$	$[10.6; +\infty [$
30	$[26.0; +\infty [$	$[14.8; +\infty [$

Table 2: Domains of full ($R > 0.998$) synchronization in the ring of nearest neighbors coupled nonidentical oscillators. Parameters of the system are (i) $\mu = 0.1$, $\alpha = 0.1$, $\beta = 0.1$; (ii) $\mu = 0.1$, $\alpha = 0.114$, $\beta = 0.005$. The spread of the frequencies is $\Delta\omega_o = 0.05$.

Figure 8 shows the stability diagram in the (N, K) plane and reveals the boundary between phase synchronization (defined as $R > 0.998$) and disordered steady-state. These curves also show that the dynamical states depend on the ring size. Analyzing the effects of the disorder parameter $\Delta\omega_o$ (that controls the spread of the frequencies of the uncoupled oscillators) on various dynamical states in the ring, one finds that such disorder parameter can also induce de-synchronization, *i.e.* even preparing the oscillators with identical initial conditions, the spread induces a disordered state.

V. AN OPEN-ENDED CHAIN OF NEAREST NEIGHBORS COUPLED OSCILLATORS

A. A chain of open-ended nearest neighbors coupled identical oscillators

N	Domains of K for stable synchronization (i)	Domains of K for stable synchronization (ii)
2	$] -0.5; -0.01[\cup] 0.014; +\infty [$	$] -0.5; -0.01[\cup] 0.009; +\infty [$
3	$] -0.34; -0.02[\cup] 0.02; +\infty [$	$] -0.334; -0.019[\cup] 0.019; +\infty [$
4	$] -0.3; -0.03[\cup] 0.04; +\infty [$	$] -0.3; -0.03[\cup] 0.03; +\infty [$
5	$] -0.28; -0.05[\cup] 0.07; +\infty [$	$] -0.28; -0.05[\cup] 0.05; +\infty [$
6	$] -0.27; -0.07[\cup] 0.1; +\infty [$	$] -0.27; -0.07[\cup] 0.07; +\infty [$
8	$] -0.26; -0.13[\cup] 0.18; +\infty [$	$] -0.26; -0.13[\cup] 0.12; +\infty [$
10	$] -0.26; -0.21[\cup] 0.29; +\infty [$	$] -0.26; -0.21[\cup] 0.19; +\infty [$
20	$] 1.16; +\infty [$	$] 0.77; +\infty [$
30	$] 2.61; +\infty [$	$] 1.74; +\infty [$
40	$] 4.66; +\infty [$	$] 3.1; +\infty [$
50	$] 7.28; +\infty [$	$] 4.85; +\infty [$

Table 3: Domains of stable synchronization in the open-ended chain of nearest neighbors coupled identical oscillators obtained with the MSF approach. Parameters of the system are (i): $\mu = 0.1$, $\alpha = 0.1$, $\beta = 0.1$, (ii) $\mu = 0.1$, $\alpha = 0.114$, $\beta = 0.005$.

Not closed chains of coupled nonlinear systems, corresponding to open-ended boundary condition, are involved in many natural processes such as the swimming motion of organisms [48] and waves synchronization that occur during sensory processing in the cortex [49, 50]. In the case of small intestinal muscle, it has proved useful to simulate and attempt an analysis of long chains of oscillators [51]. There is in fact physiological evidence that a complete organ such as small intestine, comprises a very large number of smooth muscle cells organized to form self-oscillatory segments. Also, the electrical waveforms found in the canine gastrointestinal tract are very non-sinusoidal in nature, whereas research work realized in the Department of Surgery, University of Sheffield has indicated that the human duodenal signals are nearly sinusoidal [52–54]. Consequently, the nonlinear parameter μ can be assumed small to model the duodenal oscillator cells. In fact in the autonomous regime, the final limit cycle state of the van der Pol oscillator is nearest a sinusoidal behavior for small values of μ . In contrast, for large μ it develops relaxation oscillations [55, 56]. In the open-ended chain coupling configuration, one assumes that the 1^{th} and N^{th} oscillators are not interconnected. In this case, the differential equations of motion are defined as

$$\begin{aligned}
\ddot{x}_1 - \mu(1 - x_1^2 + \alpha x_1^4 - \beta x_1^6)\dot{x}_1 + x_1 &= K(x_2 - x_1), \\
\ddot{x}_i - \mu(1 - x_i^2 + \alpha x_i^4 - \beta x_i^6)\dot{x}_i + x_i &= K(x_{i+1} - 2x_i + x_{i-1}), \quad i = 2, 3, \dots, N-1 \\
\ddot{x}_N - \mu(1 - x_N^2 + \alpha x_N^4 - \beta x_N^6)\dot{x}_N + x_N &= K(x_{N-1} - x_N).
\end{aligned} \tag{13}$$

Our purpose is to recover the essential features of the stability investigation (employing the same methods of the section III and IV) to identify some general properties of an open-ended chain of nearest neighbors coupled self-sustained systems. The stability of the synchronization process is again found following the MSF approach. In the present case, the coupling matrix is

$$\mathbf{G}_{OE} = \begin{pmatrix} -1 & 1 & 0 & \dots & 0 \\ 1 & -2 & 1 & \dots & 0 \\ 0 & 1 & -2 & \dots & 0 \\ \vdots & \vdots & \vdots & \ddots & \vdots \\ 0 & 0 & \dots & 1 & -1 \end{pmatrix}.$$

N	Domains of K for stable synchronization in the ring	Domains of K for stable synchronization in the open-ended chain
10	$] -0.24; -0.03[\cup] 0.06; +\infty [$	$] -0.25; -0.22[\cup] 0.3; +\infty [$
20	$] -0.24; -0.12[\cup] 0.22; +\infty [$	$] 1.17; +\infty [$
30	$] 0.49; +\infty [$	$] 2.62; +\infty [$
40	$] 0.87; +\infty [$	$] 4.66; +\infty [$
50	$] 1.35; +\infty [$	$] 7.28; +\infty [$

Table 4: Comparison between stability domains in the ring and the open-ended chain of identical oscillators obtained with the MSF approach, case (i): $\mu = 0.1$, $\alpha = 0.1$, $\beta = 0.1$.

The coupling matrix \mathbf{G}_{OE} also obeys the zero sum condition, and the synchronization manifold \mathcal{M} is an invariant set. Therefore, stability of the synchronous state reduces to find the behaviors of the system dynamical properties along directions in phase that are transverse to the synchronization manifold. The stability of the resulting dynamical states can be determined considering the set of variational equations (6). In Ref. [32], it was showed that the matrix \mathbf{G}_{OE} can be diagonalized in a manner similar to the shift-invariant case using a discrete Fourier transform with N replaced by $2N$, and the eigenvalues are $\gamma_k = -4 \sin^2(\pi k/2N)$, for $k = 0, 1, \dots, N-1$. This is similar to the case of diffusively coupled self-sustained systems, except that there are no degenerate modes and the highest wavelength corresponds to $k = N-1$. Nonetheless, because of the dependence of the eigenvalues on N , we will see the same dynamical states as before. The stability boundaries of the synchronization derived through the MSF are shown in the Table 3:

The dependence of the size of a chain also apparent in Fig. 9, where the MSF is plotted in the plan (K, N) for the open-ended chain. It appears that, analogously to the results reported in Fig. 2, as the size of a chain increases, the domain of stable synchronization reduces more quickly than in the case of the closed end model, see Table 4.

In Fig. 10 we plot the stability diagram in the (N, K) plane for the open-ended chain of coupled self-sustained oscillators, obtained through the MSF and a direct numerical simulations of the differential equations (13). Comparison with the case of the ring, (see Fig. 3), reveals that the agreement between the results obtained from the MSF and those of a direct numerical simulation is very good. It also indicates that the region of stable synchronization is smaller then in the case of the ring, as reported in Tables 4 and 5.

N	Domains of K for stable synchronization in the ring	Domains of K for stable synchronization in the open-ended chain
10	$[-0.24; -0.04] \cup [0.04; +\infty [$	$] -0.25; -0.21] \cup [0.2; +\infty [$
20	$[-0.24; -0.12] \cup [0.13; +\infty [$	$] 0.78; +\infty [$
30	$[0.29; +\infty [$	$] 1.75; +\infty [$
40	$[0.51; +\infty [$	$] 3.11; +\infty [$
50	$[0.79; +\infty [$	$] 4.86; +\infty [$

Table 5: Comparison between stability domains in the ring and the open-ended chain of coupled identical oscillators obtained with the MSF approach, case (ii): $\mu = 0.1$, $\alpha = 0.114$, $\beta = 0.005$.

Finally, let us add that the space profiles and the time dependent amplitudes in both cases of stable and unstable (or partially synchronized) states are very similar to those shown in Figs. 4 and 5, and therefore are not shown.

B. A chain of open-ended nearest neighbors coupled non-identical oscillators

In the case of an open-ended chain of nearest neighbors coupled non-identical oscillators, the chain's dynamics is given by the following set of equations:

$$\begin{aligned}
 \ddot{x}_1 - \mu_1(1 - x_1^2 + \alpha x_1^4 - \beta x_1^6)\dot{x}_1 + w_1^2 x_1 &= K(x_2 - x_1), \\
 \ddot{x}_i - \mu_i(1 - x_i^2 + \alpha x_i^4 - \beta x_i^6)\dot{x}_i + w_i^2 x_i &= K(x_{i+1} - 2x_i + x_{i-1}), \quad i = 2, 3, \dots, N-1, \\
 \ddot{x}_N - \mu_N(1 - x_N^2 + \alpha x_N^4 - \beta x_N^6)\dot{x}_N + w_N^2 x_N &= K(x_{N-1} - x_N).
 \end{aligned} \tag{14}$$

Our choice of considering non-identical coefficients is justified by the parameter spread encountered in real systems, as discussed in section IV for the ring of nearest neighbors coupled non identical self-sustained oscillators. The set of equations (14) is numerically integrated to compute the Kuramoto order parameter R , Eq. (12), versus the coupling coefficient K , to quantify the fraction of synchronized oscillators dynamics in the chain of open-ended nearest neighbors coupled non-identical oscillators.

Fig. 11 shows the variation of the Kuramoto order parameter R versus the coupling coefficient K for $N = 6$, $N = 10$, $N = 20$ and $N = 30$. Phase synchronization is found in the open-ended chain and the stability boundary depends on N . However, as the number of oscillators N increases, the open ended chain is very sensitive to the initial conditions and this dependence more pronounced when the coupling strength K becomes larger. Fig.12 shows the stability diagram for an open-ended chain of coupled nonidentical oscillators in the (K, N) plane, and it is qualitatively very similar to Fig. 8. The chain of coupled nonidentical oscillators capability to give rise to synchronization (defined again as $R > 0.998$) is appears in Fig. 12 represented in Table 6 for both the sets of parameters.

VI. CONCLUSIONS

We have studied some criteria under which the synchronization manifold is stable for a ring and an open-ended chain of nearest neighbors coupled van der Pol-like oscillators. By using the Master Stability Function, the stability

boundaries of the main synchronized states have been investigated and the obtained results have been complemented by numerical simulations. Thereby, the following findings have been captured: the threshold of the coupling strength from which the system displays a stable synchronized behavior is different for the cases of two sets of parameters, as depicted in Fig. 2. Moreover, as far as the diffusive coupling is concerned, we have found that with just the first and last mode's behavior one can characterize the stability of the system (as far as full synchronization is considered, *i.e.* neglecting clustered states). The stability boundaries of the synchronization have been derived as a function of the number of oscillators and of the coupling strength. We have found that increasing the number of oscillators, the synchronized states are unfavored, while, quite obviously, a larger coupling constant increases their stability. The non obvious result is the presence of a stable synchronization manifold even for *negative* values of the coupling K , *i.e.* for repulsive *interaction*. We have also found that, when the size of the ring and the coupling coefficient increases, the domains of instability become very large and the gap between analytical and numerical analysis becomes more relevant.

In the case of non identical oscillators, we have performed numerical simulations to compute the fraction of entrained oscillators by means of the Kuramoto order parameter. Varying the coupling strength, we have retrieved the region of unstable and stable synchronization states of the ring and an open ended chain of non-identical nearest neighbors coupled self-sustained oscillators. In particular, we have found that synchronization is robust enough to survive also in presence of some amount of disorder. However, the process depends upon the number of oscillators and the amount of disorder.

Research might be extended in several directions. For example we think that an extension of the analytic treatment to find stability of synchronous states in the ring of identical and non identical coupled oscillators in the presence of noise is an interesting task which can be tackled also using the Kuramoto order parameter. Also, we have restricted our research to a region of the parameters where only monorhythmic states are present. An interesting question is therefore the influence of two stable orbits on the synchronization properties in presence of disorder. Moreover, the spontaneous transition frequencies in the ring with external random excitation, such as noise, can be also experimentally observed if one can resolve in time enzymatic reactions or electronic circuits.

Acknowledgements

R.YAMAPI undertook this work with the support of the ICTP (International Centre for Theoretical Physics) Programme for Training and Research in Italian Laboratories, Trieste, Italy. He also acknowledges the support of the Laboratorio Regionale CNR/INFM at the Dipartimento di Fisica, Università di Salerno (Italy).

-
- [1] Pikovsky, A., Roseblum, M., Kurths, J.: Synchronization: A Universal Concept in Nonlinear Systems. Cambridge University Press. UK. (2001)
 - [2] Boccaletti, S., Kurths, J., Valladares, D.L., Osipov, G., Zhou, C.S.: The synchronization of chaotic systems. *Phys. Rep.* **366**(1), 1-101 (2002)
 - [3] Manrubia, S.C., Mikhailov, A.S., Zanette, A.H.: Emergence of Dynamical Order. World Scientific, Singapore (2004)
 - [4] Pecora, L.M., Carroll, T.L.: Master Stability Functions for Synchronized Coupled Systems. *Phys. Rev. Lett.* **80**, 2109-2112 (1998)
 - [5] Barahona, M., Pecora, L.M.: Synchronization in Small-World Systems. *Phys. Rev. Lett.* **89**, 054101 (2002)
 - [6] Hu, G., Yang, J., Liu, W.: Instability and controllability of linearly coupled oscillators: Eigenvalue analysis. *Phys. Rev. E* **58**, 4440-4453 (1998).
 - [7] Zhan, M., Hu, G., Yang, J.: Synchronization of chaos in coupled systems. *Phys. Rev. E* **62**, 2963-2966 (2000)
 - [8] Chen, Y., Rangarajan, G., Ding M.: General stability analysis of synchronized dynamics in coupled systems. *Phys. Rev. E* **67**, 026209 (2003)
 - [9] Kaiser, F.: Coherent oscillations in biological systems: Interaction with extremely low frequency fields. *Radio Science* **17** (5S), 17S-22S (1982).
 - [10] Decroley, O., Goldbeter, A.: Birhythmicity, chaos, and other patterns of temporal self-organization in a multiply regulated biochemical system. *Proc. Natl. Acad. Sci. U.S.A.* **79**, 6917-6921 (1982).
 - [11] Goldbeter, A.: Biochemical Oscillations and Cellular Rhythms. The Molecular Bases of Periodic and Chaotic Behaviour. Cambridge University Press, Cambridge (1996) .
 - [12] Winfree, A.T.: The Geometry of Biological Time. Springer, New York (2001);
Murray, J.D.: Mathematical Biology. Springer, Berlin (1993).
 - [13] Goldbeter, A.: Computational approaches to cellular rhythms. *Nature*, **420**, 238-245 (2002).
 - [14] Kaiser, F., Eichwald, C.: Bifurcation Structure of a Driven multiple-limit-cycle Van der Pol oscillator (I): The superharmonic resonance structure. *Int J Bifurcat Chaos* **1** 485-491 (1991)
Eichwald, C., Kaiser, F.: Bifurcation Structure of a Driven multiple-limit-cycle Van der Pol oscillator (II): Symmetry-breaking crisis and intermittency. *Int. J. Bifurc. Chaos* **1** 711-715 (1991)
 - [15] Choi, J.D., Hwang, C.J.: An Interaction Interface for Multiple Agents on Shared 3D Display, Y. Luo (Ed.): CDVE, LNCS **3675**, pp. 71-78, Springer-Verlag Berlin Heidelberg (2005)
 - [16] Wiesenfeld, K., Colet, P., Strogatz, S.H.: Synchronization Transitions in a Disordered Josephson Series Array. *Phys. Rev. Lett.* **76**, 404-407 (1996);
Frequency locking in Josephson arrays: Connection with the Kuramoto model. *Phys. Rev. E* **57**, 1563-1569 (1998).
 - [17] Barbara, P., Cawthorne, A.B., Shitov, S.V., Lobb, C.J.: Stimulated Emission and Amplification in Josephson Junction Arrays. *Phys. Rev. Lett.* **82**, 1963-1966 (1999).
 - [18] Schenato, L., Songhwai, O.H., Sastry, S., Bose, P.: Swarm Coordination for Pursuit Evasion Games using Sensor Networks, Robotics and Automation, ICRA. Proceedings of the 2005 IEEE International Conference, 18(22) 2493 (2005)
 - [19] Richard Ivry, B., Richardson, C.T.: Temporal Control and Coordination: The Multiple Timer Model, *Brain and Cognition* **48**, 117 (2002).
 - [20] Michael Rich, W.: Heart Failure in the 21st Century: A Cardiogeriatric Syndrome, *Journal of Gerontology: MEDICAL SCIENCES*, Vol. **56A**, No. 2, M88-M96 (2001).
 - [21] Enjieu Kadji, H.G., Chabi Orou, J.B., Yamapi R., Wofo, P.: Nonlinear dynamics and strange attractor in the biological system. *Chaos, Solitons and Fractals* **32**, 862-882 (2007)
 - [22] Enjieu Kadji, H. G., Yamapi, R., Chabi Orou, J.B.: Synchronization of two coupled self-excited systems with multi-limit cycles. *CHAOS* **17**, 033113 (2007)
 - [23] Yamapi, R., Nana Nbandjo, B.R., Enjieu Kadji, H.G.: Dynamics and active control of motion of a driven multi-limit-cycle Van der Pol Oscillator. *Int. journal of Bifurcation and Chaos*, **17**(4), 1343-1354 (2007)
 - [24] Nana, B., Wofo, P.: Synchronization in a ring of four mutually coupled van der Pol oscillators: Theory and experiment. *Phys. Rev. E* **74**, 046213 (2006).
 - [25] Kuznetov, A.P., Roman, J.P.: Properties of synchronization in the systems of non-identical coupled van der Pol and van der Pol - Duffing oscillators. Broadband synchronization. *Physica D* **238**, 1499-1509 (2009).
 - [26] Barrón, M.A., Sehn, M.: Synchronization of four coupled van der Pol oscillators. *Nonlinear Dynamics*, **56**, 357-367 (2009).
 - [27] Kamoun, P., Lavoine, A.H., Verneuil de, H.: Biochimie et Biologie Moléculaire, Flammarion, Paris (2003).
 - [28] Fukui, K., Nogi, S.: IEEE. *Trans. Microwave Theor. Tech.* **28**, 1059-1067 (1980).
 - [29] Fukui, K., Nogi, S.: IEEE. *Trans. Microwave Theor. Tech.* **34**, 943-951 (1986).
 - [30] Appelbe, B.: Existence of multiple cycles in a Van der Pol system with hysteresis in the inductance, *Journal of Physics: Conference Series* **55**, 1-11 (2006).
 - [31] Boccaletti, S., Latorab, V., Moreno, Y., Chavez, M., Hwang, D.-U.: Complex networks: Structure and dynamics. *Physics Reports* **424**, 175-308 (2006)
 - [32] Pecora, L. M.: Synchronization conditions and desynchronizing patterns in coupled limit-cycle and chaotic systems. *Phys. Rev. E* **58**(1), 347-360 (1998)
 - [33] Tsaneva-Atanasova, K., Yule, D.I., Sneyd, J.: Calcium Oscillations in a Triplet of Pancreatic Acinar Cells. *Biophys. J* **88**, 1535-1551 (2005)

- [34] Strogatz, S.H.: Exploring complex networks. *Nature* **410** 268-276 (2001)
- [35] Kaiser, F.: Coherent modes in biological systems. In: Illinger KH, editor. *Biological effects of nonionizing radiation*. A.C.S Symp. Series, 157 (1981).
- [36] Fröhlich, H.: Long-range coherence and energy storage in biological systems. *Int J Quantum Chem* **2**(5), 641-649 (1968); Fröhlich, H.: Quantum mechanical concepts in biology, in *theoretical physics and biology* (Marois, editor) 13 (1969).
- [37] Kuramoto, Y.: *Chemical oscillations, waves and turbulence*. Springer. Berlin (1984).
- [38] Acebrón, J.A., Bonilla, I.L., Perez Vicente, C. J., Ritrot, F., Spigler, R.: The Kuramoto model: A simple paradigm for synchronization phenomena. *Rev. Mod. Phys.* **77**, 137-185 (2005).
- [39] Arenasa, A., Daz-Guilera, A., Kurths, J., Moreno, Y., Zhou, C.: Synchronization in complex networks. *Phys. Rep.* **469**, 93-153 (2008).
- [40] Peles, S., Wiesenfeld, K.: Synchronization law for a van der Pol array, *Phys. Rev. E* **68**, 026220.1-026220.8 (2003)
- [41] Brusselbach, H., Cris Jones, D., Mangir, M.S., Minden, M., Rogers, J.L.: Self-organized coherence in fiber laser arrays. *Opt. Lett.* **30**, 1339-1341 (2005).
- [42] Strogatz, S.H., Abrams, D.M., McRobie, A., Eckhardt, B., Ott, E.: Theoretical mechanics: Crowd synchrony on the Millennium Bridge. *Nature (London)* **438**, 43-44 (2005).
- [43] Daniels, B.C., Dissanayake, S.T., Trees, B.R.: Synchronization of coupled rotators: Josephson junction ladders and the locally coupled Kuramoto model. *Phys. Rev. E* **67**, 026216 (2003).
- [44] Filatrella, G., Pedersen, N.F., Lobb, C.J., Barbara, P.: Synchronization of underdamped Josephson-junction arrays. *Eur. Phys. J. B* **34**(1), 3-8 (2003).
- [45] Dhamala, M., Wiesenfeld, K.: Generalized Stability Law for Josephson Series Arrays. *Phys. Lett. A* **292**, 269-274 (2002).
- [46] Pazó, D.: Thermodynamic limit of the first-order phase transition in the Kuramoto model. *Phys. Rev. E* **72**, 046211 (2005).
- [47] Xie, F., Hu, G.: Clustering dynamics in globally coupled map lattices. *Phys. Rev. E*, **56** 1567-1570 (1997).
- [48] Williams, T.L.: Phase coupling by synaptic spread in chains of coupled neuronal oscillators. *Science* **258**, 662-665 (1992)
- [49] Wilson, M., Bower, J.M.: Cortical oscillations and temporal interactions in a computer simulation of piriform cortex. *J. Neurophysiol* **67**(4), 981-995 (1992)
- [50] Gray, C.M., Singer, W.: Stimulus-specific neuronal oscillations in orientation columns of cat visual cortex. *Proc. Natl. aca. Sci. U.S.A.* **86**, 1698-1702 (1989)
- [51] Brown, B.H., Duthie, H.L., Horn, A.R., Smallwood, R.H.: A linked oscillator model of electrical activity of human small intestine. *Am J Physiol.* **229** (2), 384-388 (1975)
B. Robertson-Dunn, D. A. Linkens: A mathematical model of the slow wave electrical activity of the human small intestine. *Med Biol Eng.* **12**(6), 750-758 (1974)
Linkens, D.: *Circuits and Systems*, IEEE Transactions on Volume **21** (2), 294-300 (1974)
- [52] Brown, B.H., Nwong, K.K., Duthier, K.H.L., Whittaker, G. E., Franks, C.I.: *Med. Biol. Eng.* **9**, 305-314 (1971)
- [53] Duthier, H.L., Kwong, N.K., Brown, B.H., Whittaker, G.E.: *Gut* **12**, 250-256 (1971)
- [54] Duthier, H.L., Brown, B.H., Robertson-Dunn, B., Kwong, N.K., Whittaker G.E., Waterfall, W.: *Amer. J. Physiol.* **195**, 505 (1972)
- [55] van der Pol, B.: On oscillation hysteresis in a triode generator with two degrees of freedom. *Phil. Mag.* **43**(3), 700-719 (1922)
- [56] van der Pol, B.: The nonlinear theory of electric oscillations. *Proceedings of the Institute of Radio Engineers.* **22**, 1051-1086 (1934)

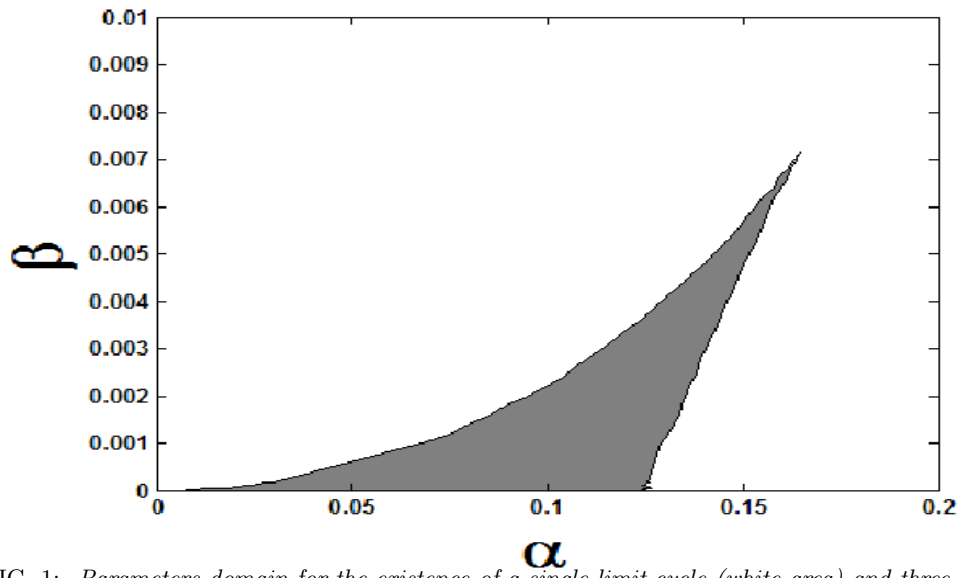


FIG. 1: Parameters domain for the existence of a single limit cycle (white area) and three limit cycles (grey area) for $\mu = 0.1$.

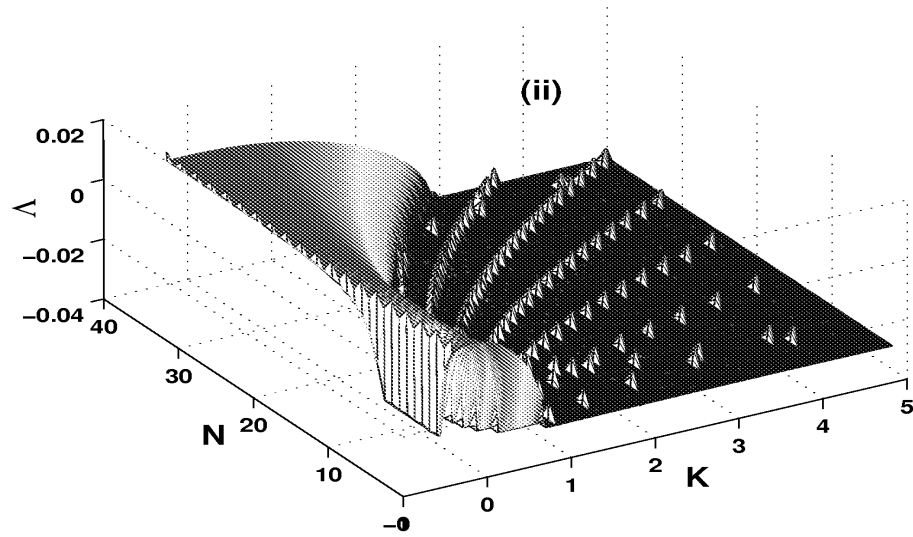


FIG. 2: Variation of the Master Stability Function (MSF) Λ versus K and N for a ring of diffusive coupling oscillators, (i) $\mu = \beta = \alpha = 0.1$ and (ii) $\mu = 0.1; \beta = 0.005, \alpha = 0.114$.

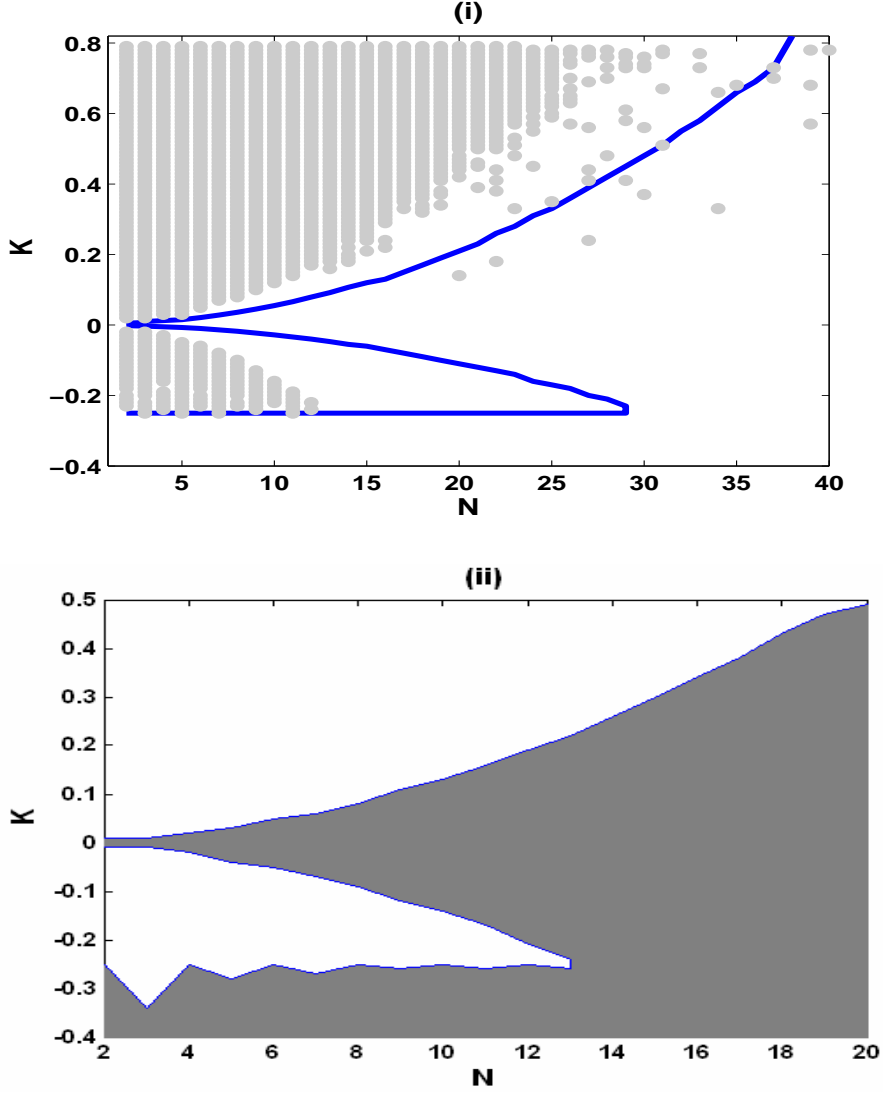


FIG. 3: Stability diagram in the (N, K) plane of a ring of diffusively coupled oscillators. The shaded area denotes the region of stable synchronization obtained numerically with $h = 10^{-6}$ (see Eq.(7)), while the solid line is the stability boundary obtained through MSF. Parameters of the system are $\mu = 0.1$; (i) $\beta = \alpha = 0.1$, (ii) $\beta = 0.005, \alpha = 0.114$.

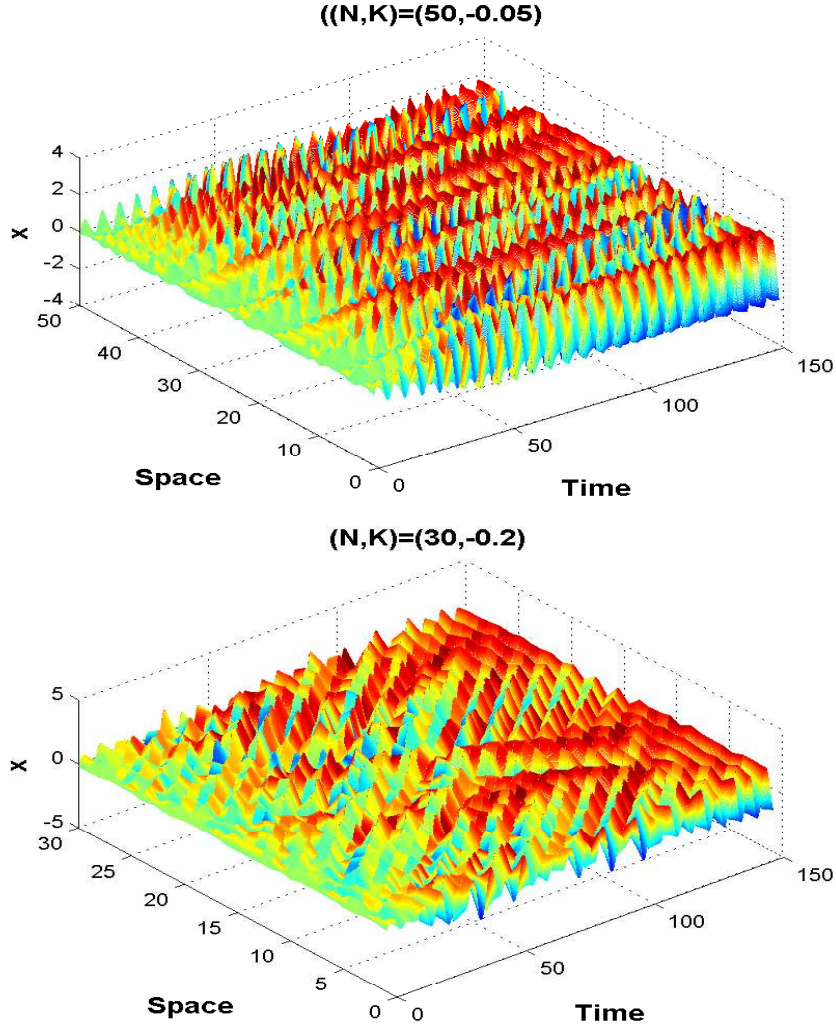


FIG. 4: *Space-time-amplitude plot showing unstable synchronization in the ring of diffusively coupled oscillators, with $\mu = \alpha = \beta = 0.1$.*

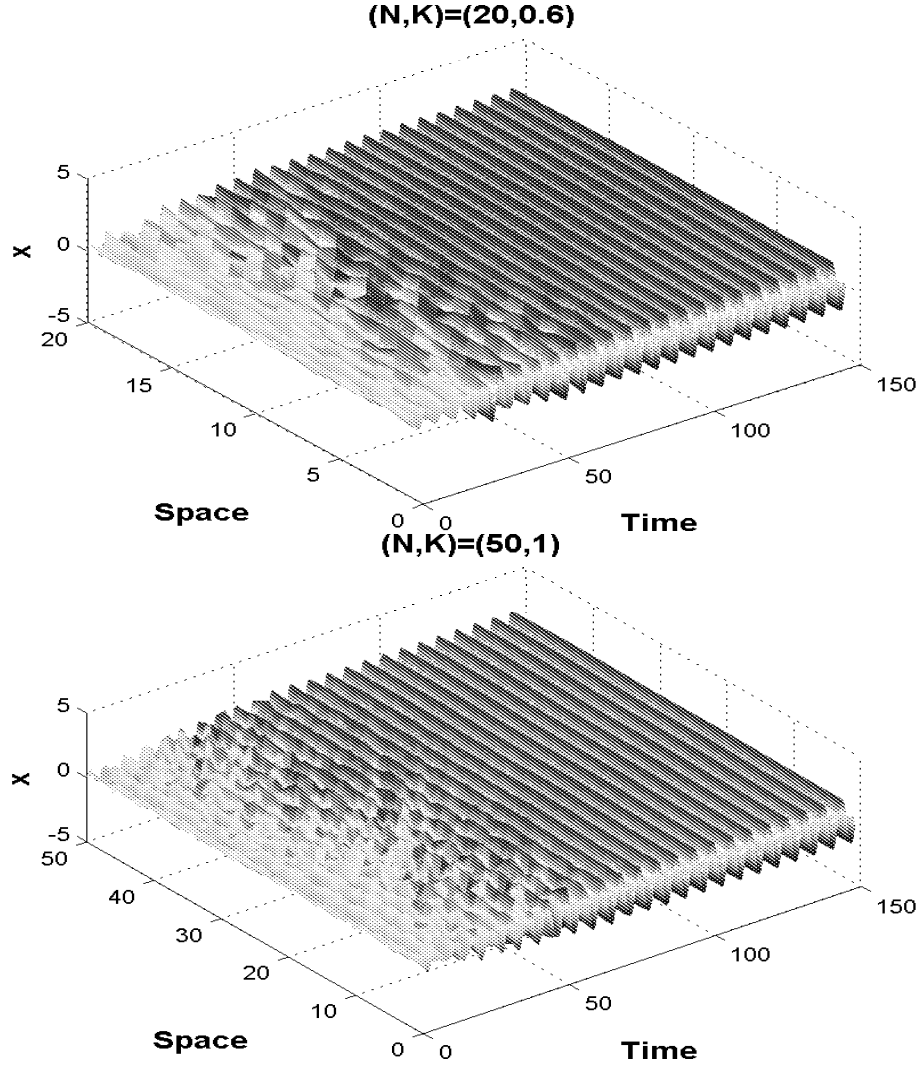


FIG. 5: Space-time-amplitude plot showing transitions from unstable to stable synchronization in a ring of diffusively coupled oscillators, with $\mu = \alpha = \beta = 0.1$.

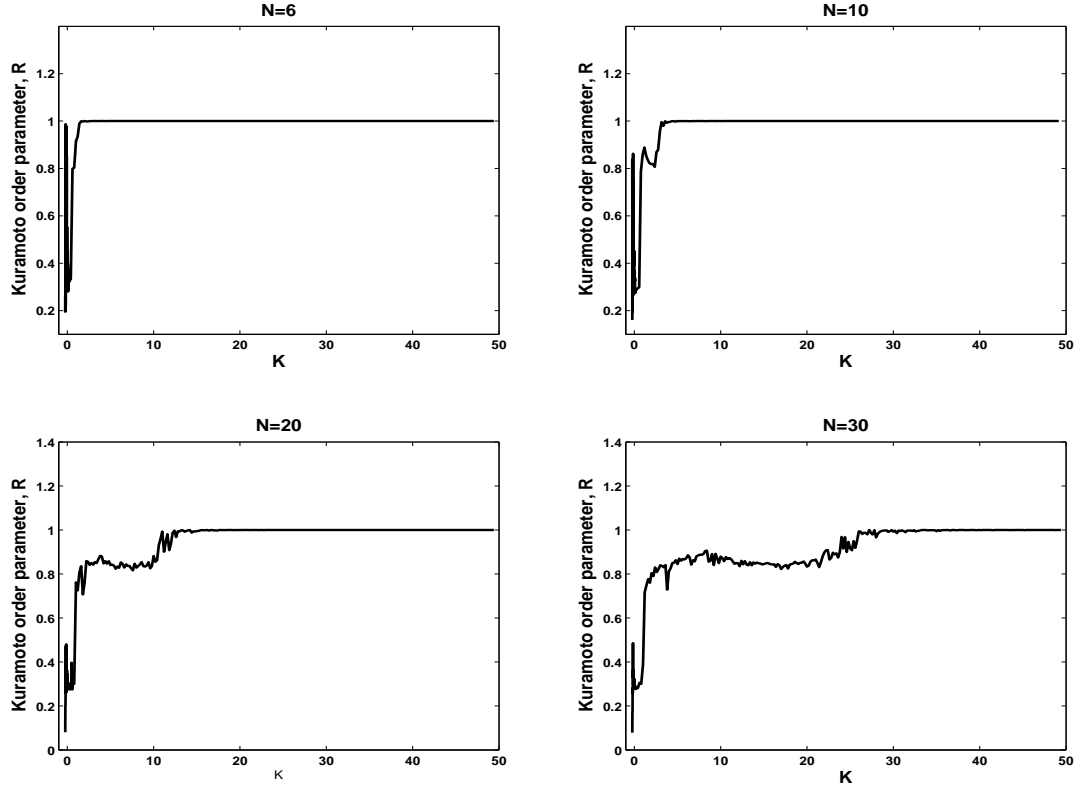


FIG. 6: Variation of the Kuramoto order parameter R versus the coupling strength K for a ring of diffusively coupled non-identical oscillators with parameters $\mu = \alpha = \beta = 0.1$, $\Delta w_o = 0.05$, $\kappa = 2$.

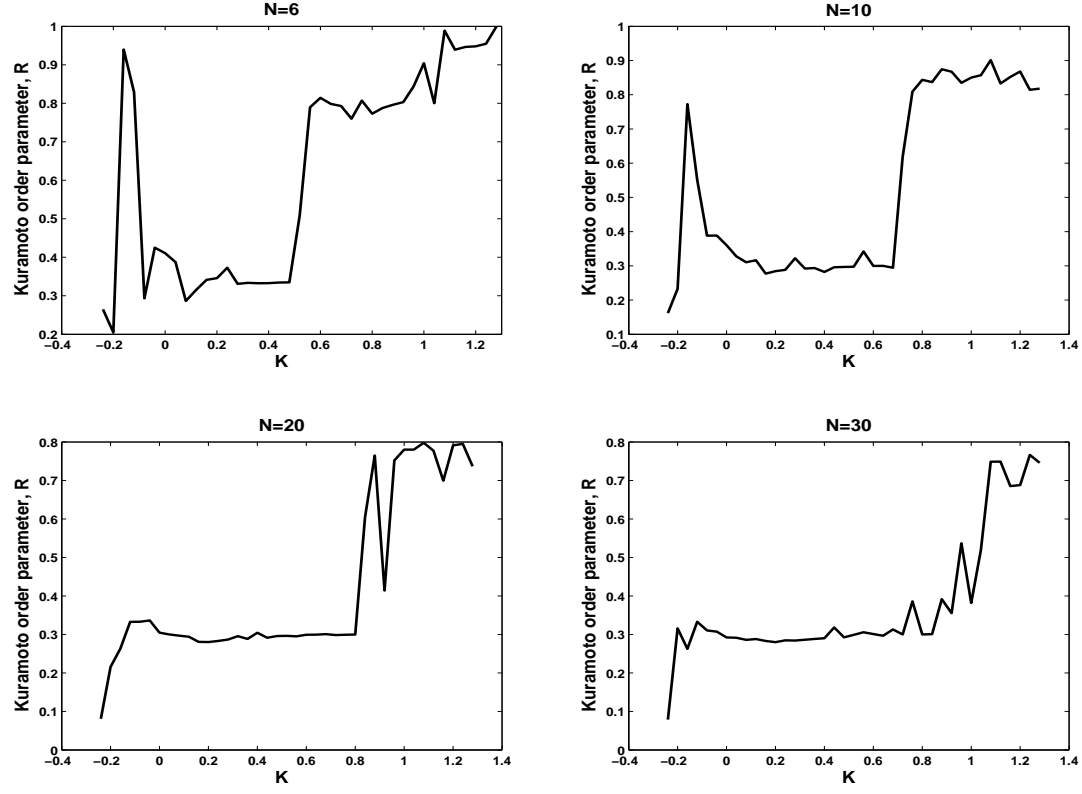


FIG. 7: Enlargement of the Kuramoto order parameter R versus the coupling strength K for the same parameters as in Fig. 6 .

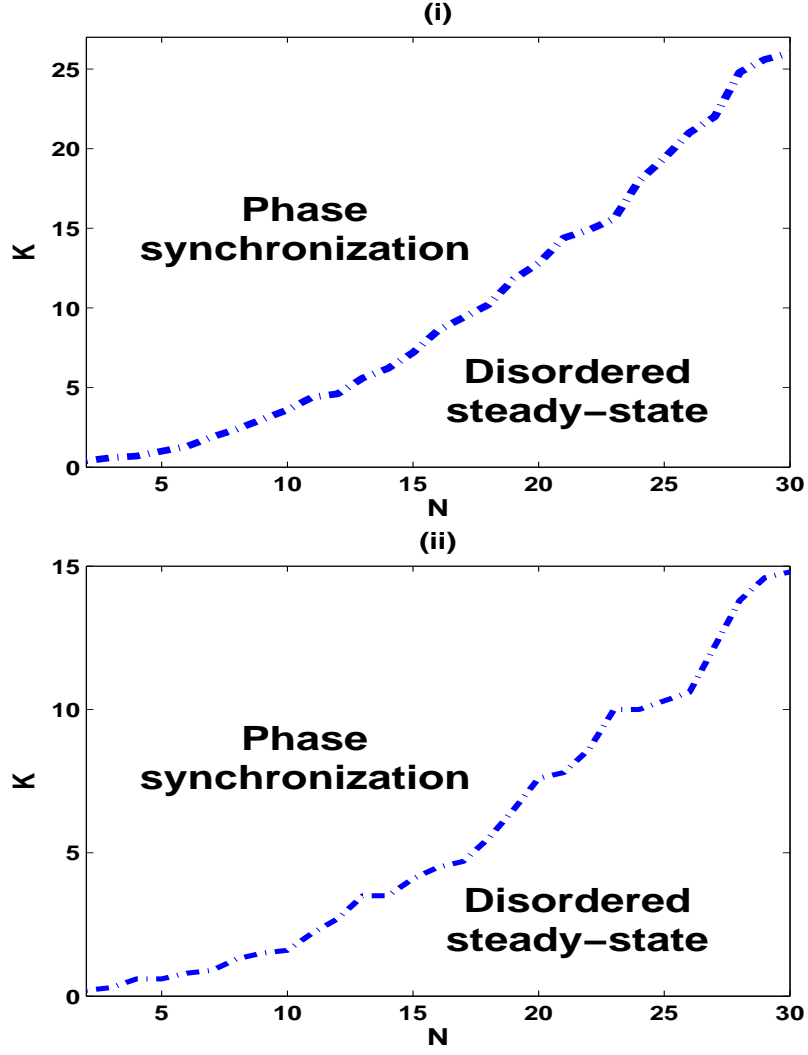


FIG. 8: Stability diagram of phase synchronization ($R > 0.998$) and disordered steady-state ($R < 0.998$) for a ring of diffusively coupled nonidentical oscillators. Parameters are $\mu = 0.1$, $\Delta w_o = 0.05$, $\kappa = 2$, (i): $\alpha = \beta = 0.1$, (ii): $\alpha = 0.114, \beta = 0.005$.

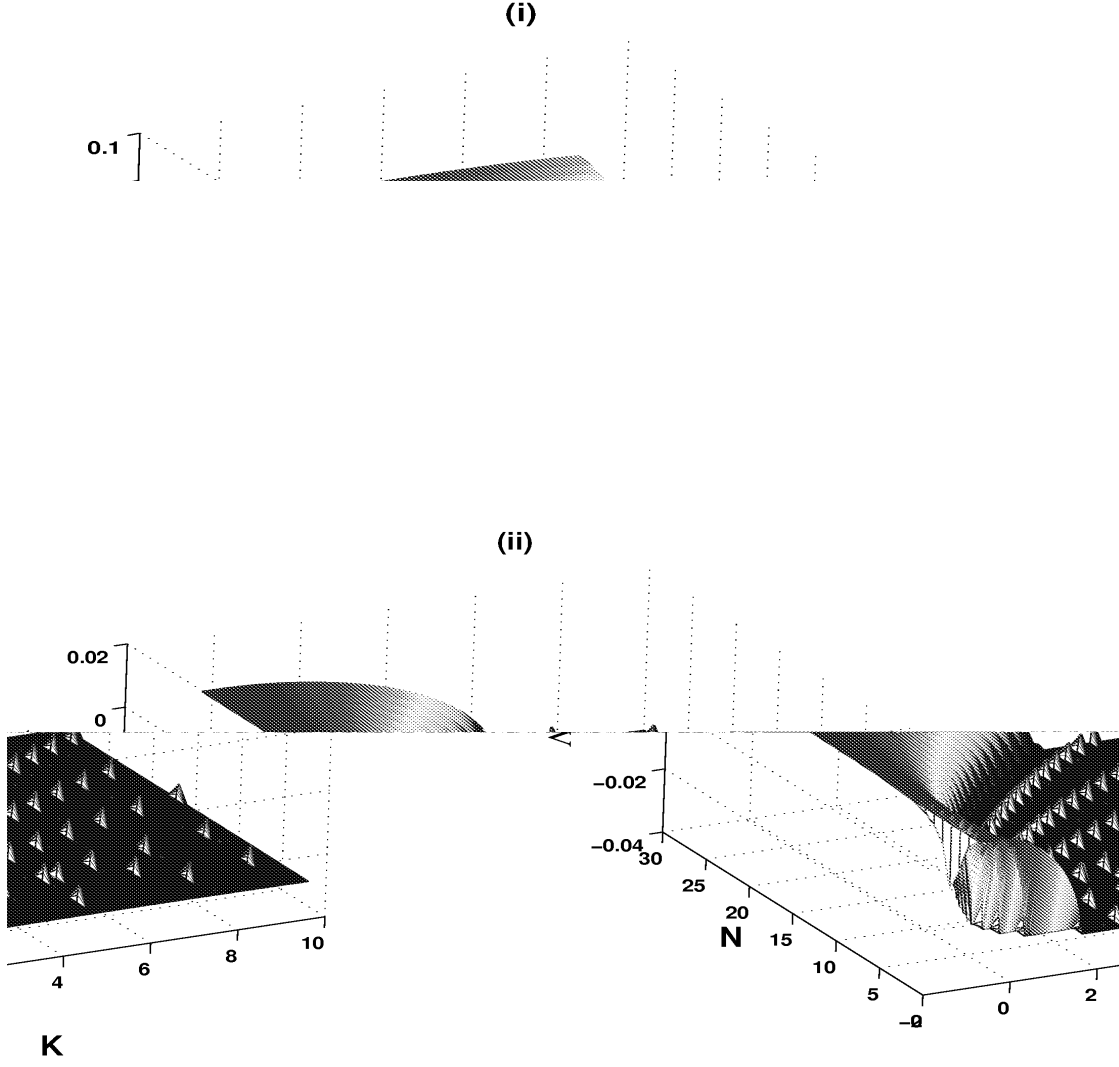


FIG. 9: Variation of the Master Stability Function (MSF) Λ versus K and N for a chain of open-ended of diffusive coupling oscillators, (i) $\mu = \beta = \alpha = 0.1$ and (ii) $\mu = 0.1; \beta = 0.005, \alpha = 0.114$.

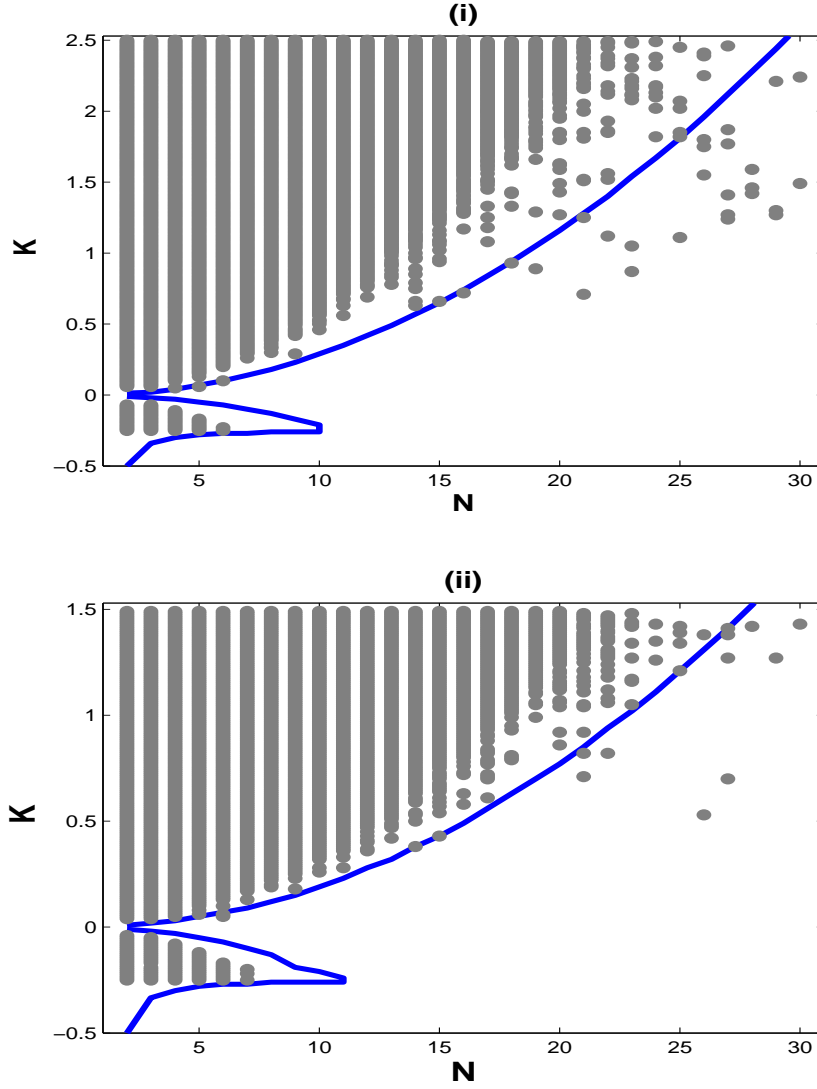


FIG. 10: Stability diagram in the (N, K) plane of chain of open ended diffusively coupled oscillators. The shaded area denotes the region of stable synchronization obtained numerically with $h = 10^{-6}$ (see Eq.(7)), while the solid line is the stability boundary obtained through the Master Stability Function (MSF). Parameters of the system are $\mu = 0.1$; (i) $\beta = \alpha = 0.1$, (ii) $\beta = 0.005, \alpha = 0.114$.

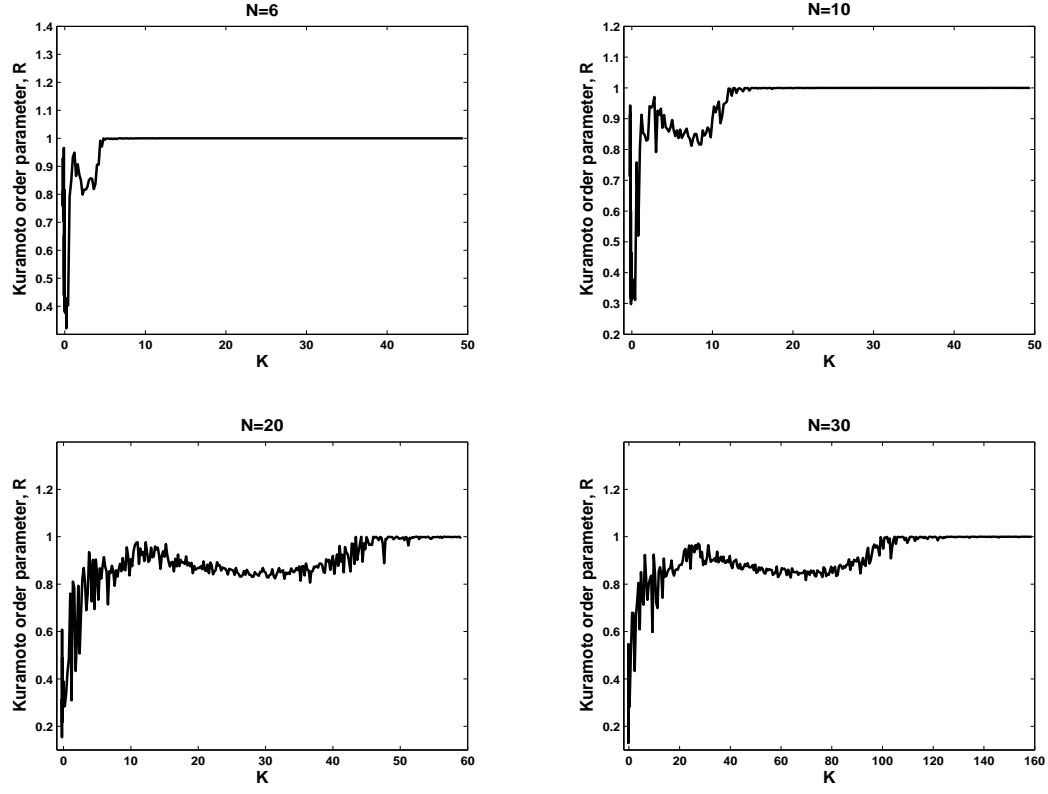


FIG. 11: Kuramoto order parameter R versus the coupling strength K for a chain of open-ended diffusively coupled non-identical oscillators with parameters $\mu = \alpha = \beta = 0.1$, $\Delta w_o = 0.05$, $\kappa = 2$.

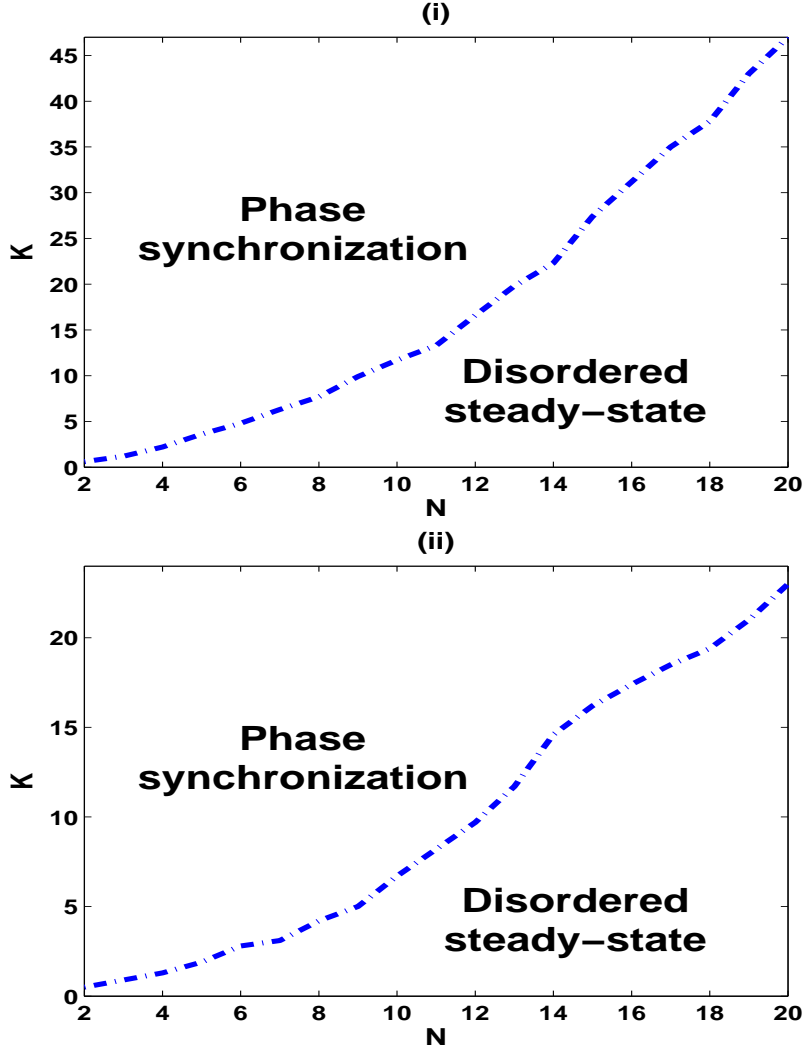


FIG. 12: Stability diagram of phase synchronization ($R > 0.998$) and disordered steady-state ($R < 0.998$) for an open-ended chain of diffusively coupled nonidentical oscillators. Parameters are $\mu = 0.1$, $\Delta w_o = 0.05$, $\kappa = 2$, (i): $\alpha = \beta = 0.1$, (ii): $\alpha = 0.114, \beta = 0.005$.